RSC Advances

PAPER

View Article Online
View Journal | View Issue



Cite this: *RSC Adv.*, 2017, **7**, 16087

# Novel alkyl chain-based fluorescent probes with large Stokes shifts used for imaging the cell membrane and mitochondria in different living cell lines†

Fangfang Meng, Yong Liu, Jie Niu and Weiying Lin*

Received 16th January 2017
Accepted 26th February 2017

DOI: 10.1039/c7ra00661f

rsc.li/rsc-advances

Fluorescent dyes with large Stokes shifts play a key role in developing multi-purpose fluorescent probes for a wide variety of targets. In this study, we developed two novel alkyl chain-based fluorescent probes (**CA-C12** and **CA-C2**) with large Stokes shifts. The alkyl chain length of the probes affect the membrane permeability, and hence both probes can be successfully applied for sensing the cell membrane and mitochondria in different living cell lines. Furthermore, the probes **CA-C12** and **CA-C2** exhibited large Stokes shifts and excellent photostability in the different cell lines. The fluorescent dyes with large Stokes shifts were expected to have broader applications for developing various fluorescent probes with excellent optical properties.



## Introduction

The cell membrane is selectively permeable to various biological analyses and controls the movement of substances in and out of cells.[1] The cell membrane covers the cytoplasm of living cells, physically separating the intracellular components from the extracellular environment.[2] The cell membrane can regulate what enters and exits the cell, facilitating the transport of materials needed for survival.[3] The cell membrane plays a key role in cell signal transduction and solute transporting.[4–6] In addition, it plays an important role in anchoring the cell cytoskeleton and its attachment to the extracellular matrix and more cells to form tissues.[7–9] Consequently, the search for a method of monitoring the cell membrane has always been attractive.

Mitochondria is also a membrane organelle and plays a key role in energy production through respiratory chains,[10–12] cell signalling *via* the production of reactive oxygen species,[13,14] the regulation of $Ca^{2+}$ homeostasis,[15,16] and triggering cell death.[17–20] Mitochondrial dysfunction is associated with intrinsic apoptotic pathways and causes a variety of neurodegenerative diseases including Alzheimer's disease, cancer and diabetes.[21–23] Therefore, it is of importance to image mitochondria in biological samples.

Compared to conventional technology, fluorescent probes have become powerful tools for detecting various targets in the environment, chemistry and medicine.[24–26] Recently, a wide variety of fluorescent cell membrane and mitochondria probes have been engineered,[27,28] but most of the cell membrane and mitochondria probes possessed small Stokes shifts; however, a small Stokes shift leads to fluorescence imaging errors of the probes in biological applications.[29] Thus, the goal of our study is to design cell membrane and mitochondria probes with large Stokes shifts for imaging the cell membrane and mitochondria in different living cell lines.

As we know, carbazole derivatives show a number of attractive features including large Stokes shifts and excellent optical properties.[30,31] In this study, we have developed two novel alkyl chain-based fluorescent probes (**CA-C2** and **CA-C12**) with large Stokes shifts based on a carbazole derivative (Fig. 1). It was found that both probes containing long and short alkyl chains can image the cell membrane and mitochondria in different living cell lines. We envisioned that the alkyl chain length affects the membrane permeability of the probes and indicated that the probes can real-time image the cell membrane and mitochondria in different living cell lines.

## Experimental

### Measurements equipment and materials

Unless otherwise stated, all reagents were purchased from commercial suppliers and used without further purification. Solvents were purified by standard methods prior to use. Doubly-distilled water was used throughout all the experiments. Mass spectra were recorded on a 6510 Q-TOF LC/MS or

*Institute of Fluorescent Probes for Biological Imaging, School of Materials Science and Engineering, School of Chemistry and Chemical Engineering, University of Jinan, Shandong 250022, P. R. China. E-mail: weiyinglin2013@163.com*

† Electronic supplementary information (ESI) available: Experimental procedure, fluorescence spectra, tables and characterization data. See DOI: 10.1039/c7ra00661f

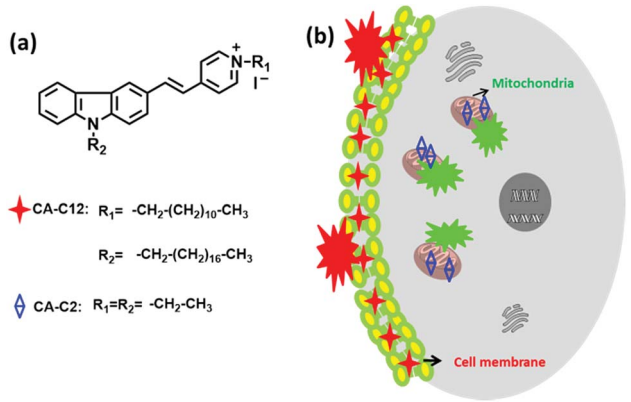


Fig. 1 (a) The structures of the probes CA-C2 and CA-C12, and (b) the overall strategy using probes CA-C2 and CA-C12 for imaging the cell membrane and mitochondria, respectively.

ThermoFisher LCQ FLEET. NMR spectra were recorded on a Bruker Avance 400 spectrometer using TMS as an internal standard. The UV-visible-near-IR absorption spectra were obtained on a Labtech UV Power PC spectrometer. Photoluminescent spectra were recorded on a HITACHI F-4600 fluorescence spectrophotometer with the excitation and emission slit widths at 5.0 and 5.0 nm, respectively. Fluorescence imaging of the cells was performed using a Nikon A1MP two-photon confocal microscope. TLC analysis was performed on silica gel plates and column chromatography was conducted over silica gel (mesh 200–300), both of which were purchased from the Qingdao Ocean Chemicals. HeLa cells, A549 cells, 4T-1 cells and calf serum were obtained from the College of Life Science, Nankai University (Tianjin, China).

### Measurement of the fluorescence quantum yield

The fluorescence quantum yields ($\Phi$) were calculated using eqn (1):

$$\Phi_s = \Phi_r \left(\frac{A_r}{A_s}\right)\left(\frac{{n_s}^2}{{n_r}^2}\right)\frac{I_s}{I_r} \quad (1)$$

In this equation, the subscripts s and r refer to the sample and the reference molecule, respectively. $A$ is the absorbance of the molecules for both the sample and reference. $I$ represents the integrated emission area and $n$ is the refractive index of the solvent. $\Phi$ is the quantum yield.

### Preparation of the test solutions

Stock solutions of the probes **CA-C2** and **CA-C12** were prepared at 1 mM in DMF. Different solvents were used, including PBS, $H_2O$, $CHCl_3$, DCM, DMF, DMSO, EtOH, MeOH, MeCN and THF. Test solutions of the probes **CA-C2** and **CA-C12** (10 μM) in 5 mL of the different solvents were prepared. For the fluorescence spectra experiments, the excitation wavelength was 421 nm and the emission slit widths were 5 nm and 5 nm.

### Cell culture and imaging

Different types of cells (A549, 4T-1 and HeLa) were grown in Dulbecco's modified Eagle's medium, high glucose supplemented with penicillin/streptomycin and 10% FBS in a 5% $CO_2$ incubator at 37 °C. Before the imaging experiments, the cells were cultured overnight on a 35 mm Petri dish in order for their convenient observation. Cells were incubated with 10 μM **CA-C2** and **CA-C12** for 10 min at 37 °C, respectively. After being washed twice with PBS, the cells were imaged immediately. In the co-localization experiment, different cells were incubated with 2 μM commercially available mitochondrial probe MitoTracker Red (MTR) for 20 min; after being washed three times with PBS, 10 μM **CA-C2** was added to the cells and incubated for 10 min. Then, the cells were washed three times using PBS before imaging with a Nikon fluorescence microscope.

### Cell viability evaluated by MTT

We used the colorimetric methyl cytotoxicity assay thiazolyl tetrazolium (MTT) assay on HeLa cells to measure *in vitro* cytotoxicity. About six thousand cells were seeded per well in a 96-well plate. After being incubated for 24 h, different concentrations (0, 1, 5, 10, 20 and 30 μM) of the probes were added into each well. After 8 h of incubation, the cells were washed. Subsequently, 100 μL of MTT (5 mg $mL^{-1}$) was added to each well and further incubated for 4 h. After removing the medium, 100 μL of DMSO was added to each well to dissolve the purple crystals. Then, the absorbance at 570 nm was measured using a microplate reader.

## Results and discussion

### Preparation of probe

The chemical syntheses of **CA-C2** and **CA-C12** were accomplished in a total of four steps (Scheme 1). *N*-(2-Ethyl/dodecyl)-4-

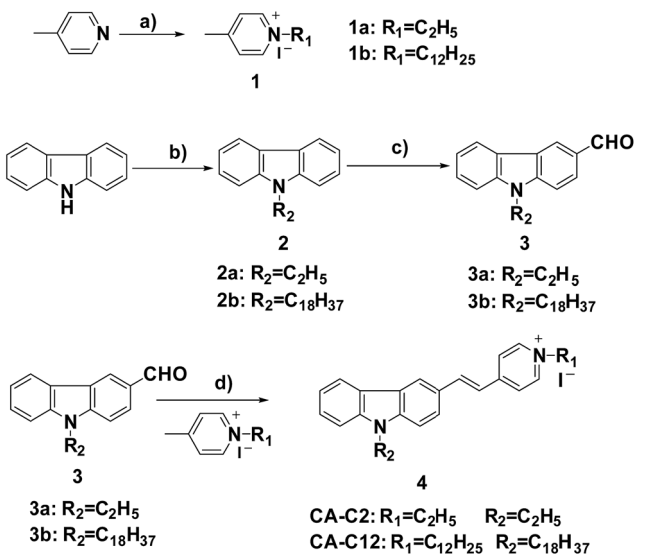


Scheme 1 The synthesis of the probes: (a) 1-bromooctadecane/bromoethane, KOH, DMF, (b) DMF, $POCl_3$ and $CHCl_3$, (c) 1-iodoundecane/iodoethane, EtOH, reflux and (d) EtOH, reflux.

methylpyridinium iodide (**1**) and 9-ethyl/octadecyl-9*H*-carbazole (**2**) were prepared *via* an alkylation reaction. 9-Ethyl/octadecyl-9*H*-carbazole-3-carbaldehyde (**3**) was prepared in one step *via* the Vilsmeier reaction of compound (**2**) with phosphorus oxychloride. The target molecules **CA-C2** and **CA-C12** were obtained *via* a Knoevenagel condensation reaction between compound (**3**) and (**1**). The synthetic details of the products are given in the ESI.†

## Optical properties

To demonstrate the potential utility of **CA-C2** and **CA-C12** as suitable tracers for live-cell imaging, we evaluated the optical photophysical properties of both probes. As shown in Fig. 2 and S1,† we found that the absorbance and emission spectra of **CA-C12** was similar to **CA-C2** in various solutions. The maximum absorption of **CA-C12** and **CA-C2** was 430 nm (Fig. 2a and S1a†) and 440 nm (Fig. 2c and S1c†), respectively. **CA-C12** and **CA-C2** have an emission peak at 570–605 nm in various solutions, but the fluorescence intensities were very high in organic solvents compared to those in an aqueous solution (Fig. 2b, d, S1b and d†). The results demonstrate that compounds **CA-C12** and **CA-C2** exhibited large Stokes shifts in various solutions (Table 1), which results in an efficient separation of the absorbance and emission maxima. The quantum yield ($\Phi$) of the probes **CA-C12** and **CA-C2** was only 0.01–0.04 in an aqueous solution. In organic solvents, however, the maximum quantum yield of both probes reached 0.10–0.20 (Table 1).

As we know, mitochondria and the cell membrane are composed of different organic phases. Thus, we think that probes **CA-C12** and **CA-C2** may show strong fluorescence in the mitochondria or cell membrane. In addition, we further investigated the water solubility of the probes.[32] The solubility of **CA-C12** and **CA-C2** in water was 1.26 μM and 3.6 μM, respectively. The results demonstrated that probe **CA-C12** exhibited higher hydrophobicity than **CA-C2** (Fig. S2†). Over a wide physiological pH range from 4.0 to 8.0, the probes were found to be weakly fluorescent (Fig. 3), which demonstrated that **CA-C12** and **CA-C2** were not affected by pH.

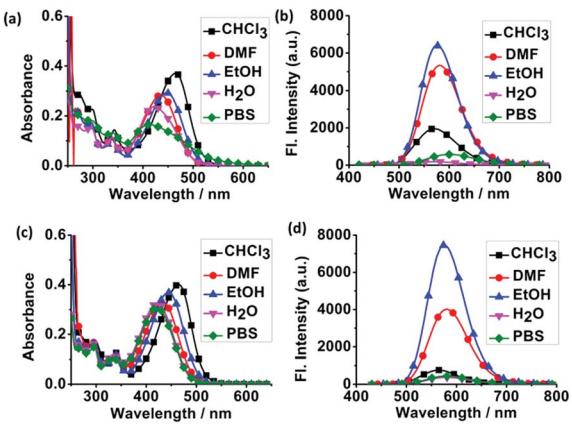


Fig. 2 The absorption and fluorescence spectra of **CA-C12** (a and b) and **CA-C2** (c and d) in various solvents. $CHCl_3$ (■), DMF (●), EtOH (▲), $H_2O$ (▼) and PBS (◆). [**CA-C12**] = [**CA-C2**] = 10 μM.

Table 1 The photophysical properties of **CA-C12**/**CA-C2** in various solvents

| | **CA-C12** | | | **CA-C2** | | |
|---|---|---|---|---|---|---|
| Sample | $\lambda_a{}^a/\lambda_b{}^b$ (nm) | SS[c] (nm) | $\Phi_d$/% | $\lambda_a{}^a/\lambda_b{}^b$ (nm) | SS[c] (nm) | $\Phi_d$ (%) |
| PBS | 410/605 | 195 | 3.56 | 421/581 | 160 | 1.4 |
| $H_2O$ | 420/573 | 153 | 0.73 | 421/582 | 161 | 1.1 |
| $CHCl_3$ | 465/570 | 105 | 4.8 | 465/564 | 99 | 1.6 |
| DCM | 473/578 | 105 | 15 | 470/575 | 105 | 9.6 |
| DMF | 430/580 | 150 | 16 | 433/580 | 147 | 11 |
| DMSO | 432/583 | 151 | 15 | 431/580 | 149 | 20 |
| EtOH | 445/575 | 130 | 18 | 444/576 | 132 | 18 |
| MeOH | 442/578 | 136 | 13 | 437/575 | 138 | 11 |
| MeCN | 437/582 | 145 | 10 | 443/574 | 131 | 13 |
| THF | 437/576 | 139 | 18 | 434/576 | 142 | 14 |

[a] Maximum absorption wavelength (nm). [b] Maximum emission wavelength (nm). [c] Stokes shift (SS). $\Phi_d$ is the fluorescence quantum yield (error limit: 8%) determined using fluorescein ($\Phi$ = 0.95) in aqueous NaOH (pH 13) as the standard.

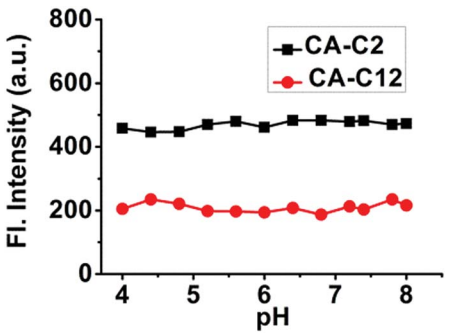


Fig. 3 The intensity of probes **CA-C12** and **CA-C2** in a buffer solution at different pH values. Excitation wavelength: 405 nm. [**CA-C12**] = [**CA-C2**] = 2 μM.

## Cell membrane imaging and photostability

To investigate the imaging of **CA-C12** in living cell lines, fluorescence imaging experiments were carried out. The cytotoxicity was evaluated using standard MTT assays, indicating that the probe **CA-C12** showed low toxicity to the cultured cells under the experimental conditions (Table S1†). Cancer cells (A549, 4T-1 and HeLa cells) were incubated with **CA-C12** for 10 min, followed by fluorescence microscopy. As shown in Fig. 4, the results of cells imaging demonstrated that the **CA-C12** was located in the cell membrane and the probe was a cell membrane probe with poor permeability.

The photostability is one of the most important criteria for constructing novel fluorescence probes.[33–36] Continuous scanning using a Nikon AMP1 confocal microscope was used to quantitatively investigate the photostability of **CA-C12** (10 μM). Within 360 s, the fluorescence signals of **CA-C12** decreased slightly in living HeLa cells (Fig. 5) and other living cells lines (Fig. S3†). The results proved that the probe **CA-C12** was capable of real-time imaging cells membrane in different cell lines.

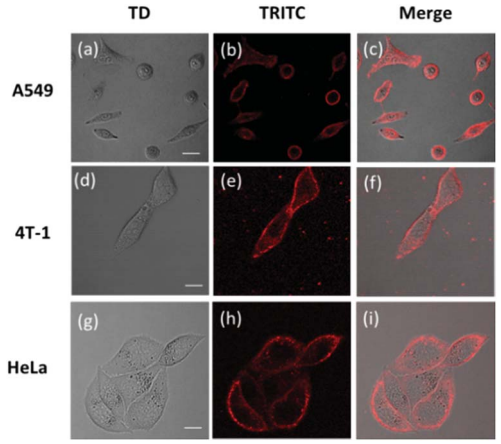


Fig. 4 (a–i) Confocal images of the probe **CA-C12** (10 μM) in different cells lines. (a, d and g) Bright-field images, (b, e and h) fluorescence images of **CA-C12** to the cell membrane ($\lambda_{ex}$ = 405 nm; $\lambda_{em}$ = 570–620 nm) and (c, f and i) merged images. Scale bar = 20 μm.

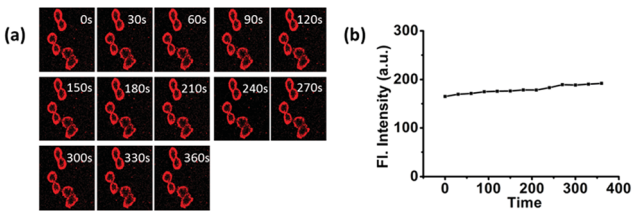


Fig. 5 (a) Fluorescence images (the red channel) of Hela cells incubated with **CA-C12** acquired at different times under successive excitation. (b) The mean intensities of the cells incubated with **CA-C12** (10 μM) in the red channel under successive excitation at different times. Excitation wavelength: 405 nm.

## Mitochondria imaging and photostability

Contrary to the probe **CA-C12** with a long alkyl chain, **CA-C2** should possess superior permeability. Subsequently, we investigated whether **CA-C2** can enter cells and image the mitochondria. Similarly, the cytotoxicity of **CA-C2** was evaluated by MTT assays (Table S1†) and the data proved that **CA-C2** had low toxicity towards living cells. As shown in Fig. 6, the probe **CA-C2** possessed superior permeability to living cells and exhibited strong fluorescence in different living cells (A549, 4T-1 and HeLa cells).

Furthermore, to prove that the probe can image the mitochondria in different living cell lines, co-localization experiments were carried out. To determine the intracellular location of **CA-C2** inside the cells, probe **CA-C2** and the commercial mitochondrial tracker MTR were co-incubated in different cell lines (Fig. 7a–l). The intensity profile of the linear regions of interest across a HeLa cell in the green and red channels also varies in close synchrony (Fig. 7j–m). The Mander's overlap coefficient and Pearson's co-localization coefficient were determined as 0.95 and 0.90, respectively (Fig. 7n). The imaging results demonstrate that probe **CA-C2** was capable of imaging the mitochondria in different living cells lines. Similar to **CA-C12**, probe **CA-C2** showed a high

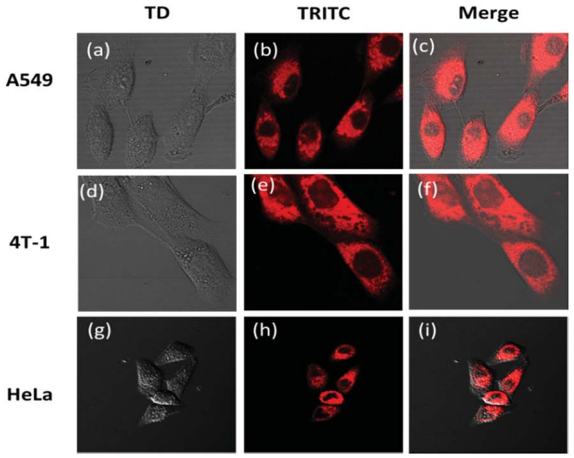


Fig. 6 (a–i) Confocal images of the different cells incubated with 10 μM probe **CA-C2**. (a, d and g) Bright-field images, (b, e and h) fluorescence images of **CA-C2** ($\lambda_{ex}$ = 405 nm; $\lambda_{em}$ = 570–620 nm) and (c, f and i) the merged images. Scale bar = 20 μm.

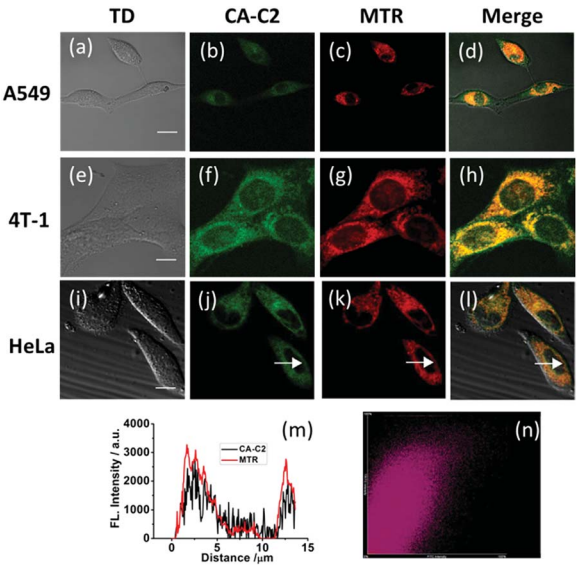


Fig. 7 The confocal images of cells treated with MTR (2 μM) for 20 min and probe **CA-C2** (10 μM) for 10 min. (a, e and i) Bright-field images, (b, f and j) fluorescence images of probe **CA-C2** collected between 500 and 550 nm upon excitation at 405 nm, (c, g and k) fluorescence images of MTR collected between 570 and 620 nm upon excitation at 561 nm and, (d, h and l) the merged images. (m) The intensity profile of the linear region of interest (white arrow) across the HeLa cells co-incubated with MTR and **CA-C2**. (n) The correlation plot of MTR and **CA-C2** intensities. Scale bar = 20 μm.

fluorescence intensity within 360 s and this feature is promising as the probe can real-time image the mitochondria over a long period of time (Fig. 8). In addition, we further proved that probe **CA-C2** possessed high photostability in living A549 and 4T-1 cells (Fig. S4†).

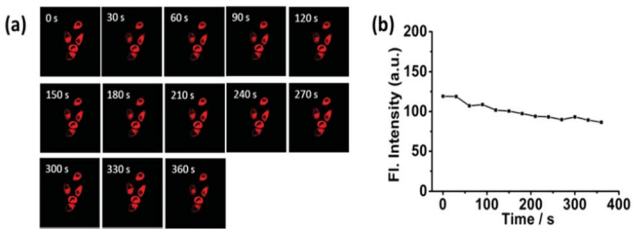


Fig. 8 (a) The fluorescence images (the red channel) of HeLa cells incubated with CA-C2 acquired at different times under successive excitation. (b) The mean intensities of the cells incubated with CA-C2 (10 μM) in the red channel under successive excitation at different times. Excitation wavelength: 405 nm.

## Conclusions

In summary, we described two novel alkyl chain-based fluorescent probes (**CA-C12** and **CA-C2**) with large Stokes shifts. The alkyl chain length of the probes affects the membrane permeability and allows both probes to be successfully applied for sensing the cell membrane and mitochondria in different living cell lines. Furthermore, probes **CA-C12** and **CA-C2** exhibited excellent photostability in different cell lines. This finding may open an avenue to engineer new fluorescent probes with improved optical properties.

## Acknowledgements

This study was financially supported by the NSFC (21472067, 21672083 and 51503077), the Taishan Scholar Foundation (TS 201511041) and the startup fund of the University of Jinan (309-10004) as well as the Doctor start up fund of University of Jinan (160082102) and NSFSP (ZR2015PE001).

## Notes and references

1 K. Simons and E. Ikonen, *Nature*, 1997, **387**, 569.
2 G. W. Feigenson, *Annu. Rev. Biophys. Biomol. Struct.*, 2007, **36**, 63.
3 L. Sherwood, *Human Physiology: From cells to systems*, West Publishing Company, New York, 1993.
4 B. Nichols, *Nature*, 2005, **436**, 638.
5 Y. Lange, J. Ye and T. L. Steck, *Biochemistry*, 2007, **46**, 2233.
6 H. Lodish, A. Berk, S. L. Zipursky, P. Matsudaira, D. Baltimore and J. Darnell, *Molecular Cell Biology*, Scientific American Book, New York, 4th edn, 2004.
7 M. R. Bernfield, S. D. Banerjee, J. E. Koda and A. C. Rapraeger, *The role of extracellular matrix in development*, New York, 1984.
8 S. K. Sastry and A. F. Horwitz, *Curr. Opin. Cell Biol.*, 1993, **5**, 819.
9 B. M. Gumbiner, *Molecular Biology of the Cell*, New York, 4th edn, 1996.
10 S. Anderson, A. T. Bankier, B. G. Barrell, M. H. L. D. Bruijin, A. R. Coulson, J. Drouin, I. C. Eperon, D. D. Nierlich, B. A. Roe, F. Sanger, P. H. Schreier, A. J. H. Smith, R. Staden and I. G. Young, *Nature*, 1981, **290**, 457.
11 S. W. Ballinger, J. M. Shoffner, E. V. Hedaya, I. Trance, M. A. Polak, D. A. Koontz and D. C. Wallace, *Nat. Genet.*, 1992, **1**, 11.
12 M. J. Bibb, V. R. A. Etten, C. T. Wright, M. W. Walberg and D. A. Clayton, *Cell*, 1981, **26**, 167.
13 N. S. E. Chandel, E. Goldwasser, C. E. Mathien, M. C. Simon and P. T. Schumacker, *Proc. Natl. Acad. Sci. U. S. A.*, 1998, **95**, 11715.
14 A. Boveris, N. Oshino and B. Chance, *Biochem. J.*, 1972, **128**, 617.
15 M. F. Rossier, *Cell Calcium*, 2006, **40**, 155.
16 R. Rizzuto, P. Pinton, W. Carrington, F. S. Fay, K. E. Fogarty, L. M. Lifshitz, R. A. Tuft and T. Pozzan, *Science*, 1998, **280**, 1763.
17 N. Patil, D. R. Cox, D. Bhat, M. Faham, R. M. Myers and A. S. Peterson, *Nat. Genet.*, 1995, **11**, 126.
18 G. Kroemer and J. C. Reed, *Nat. Med.*, 2000, **6**, 513.
19 Q. F. Ahkong, D. Fisher, W. Tampion and J. A. Lucy, *Nature*, 1975, **253**, 194.
20 D. R. Green and G. Kroemer, *Science*, 2004, **5684**, 626.
21 M. T. Lin and M. F. Beal, *Nature*, 2006, **443**, 787.
22 E. J. Lesnefsky, S. Moghaddas, B. Tandler, J. Kernerb and C. L. Hoppel, *J. Mol. Cell. Cardiol.*, 2001, **33**, 1065.
23 W. D. Parker, C. M. Filley and J. K. Parks, *Neurology*, 1990, **40**, 1302.
24 M. Y. Berezin and S. Achilefu, *Chem. Rev.*, 2010, **110**, 2641.
25 H. Kobayashi, M. Ogawa, R. Alford, P. L. Choyke and Y. Urano, *Chem. Rev.*, 2010, **110**, 2620.
26 E. L. Que, D. W. Domaille and C. J. Chang, *Chem. Rev.*, 2008, **108**, 1517.
27 Y. Xia and L. Peng, *Chem. Rev.*, 2013, **113**, 7880.
28 A. R. Sarkar, C. H. Heo, H. W. Lee, K. H. Park, Y. H. Suh and H. M. Kim, *Chem. Rev.*, 2015, **115**, 5014.
29 H. Langhals, O. Krotz, K. Polborn and P. Mayer, *Angew. Chem., Int. Ed.*, 2005, **44**, 2427.
30 N. Blouin, A. Michaud, D. Gendron, S. Wakim, E. Blair, R. N. Plesu, M. Belletete, G. Durocher, Y. Tao and M. Leclerc, *J. Am. Chem. Soc.*, 2008, **130**, 732.
31 G. Zotti, G. Schiavon, S. Zecchin, J.-F. Morin and M. Leclerc, *Macromolecules*, 2002, **35**, 2122.
32 H. M. Kim, B. H. Jeong, J.-Y. Hyon, M. J. An, M. S. Seo, J. H. Hong, K. J. Lee, C. H. Kim, T. Joo, S.-C. Hong and B. R. Cho, *J. Am. Chem. Soc.*, 2008, **130**, 4246.
33 B. P. Wittmershaus, J. J. Skibicki, J. B. McLafferty, Y. Z. Zhang and S. Swan, *J. Fluoresc.*, 2001, **11**, 119.
34 J. E. H. Buston, J. R. Young and H. L. Anderson, *Chem. Commun.*, 2000, **11**, 905.
35 B. R. Renikuntla, H. C. Rose, J. Eldo, A. S. Waggoner and B. A. Armitage, *Org. Lett.*, 2004, **6**, 909.
36 N. I. Shank, H. H. Pham, A. S. Waggoner and B. A. Armitage, *J. Am. Chem. Soc.*, 2013, **135**, 242.